Plane wave in vertically heterogeneous anisotropic media

Qi Hao and Alexey Stovas, Norwegian University of Science and Technology*

Summary

First-order velocity-stress equations for plane waves in vertically heterogeneous, anisotropic media are derived using the Radon transform. The derived plane wave equations include three particle velocity components and three z-axis related stress components. Finite-difference method is employed to simulate three-component plane wave propagation in this medium. The stationary condition is derived for proposed finite-difference scheme. Numerical examples confirm the validity of our scheme and show that it can be used to synthesize multi-component plane wave VSP seismograms. The potential applications of the plane wave modeling include AVA analysis and waveform inversion for vertically heterogeneous anisotropic media.

Introduction

It is well known that the study on plane wave propagation in anisotropic media plays an important role in many aspects of seismic exploration, such as amplitude variation versus angle (AVA) analysis, and forward modeling used in inversion procedure. The plane wave seismic data may be obtained through applying the Radon transform to 2D or 3D seismic data.

For the homogeneous anisotropic media, the analytical plane wave solution has been obtained by Cerveny (2001). However, it is very difficult to get the analytical solutions for complex media. Semi-analytical methods such as the propagator matrix can be used to calculate the response of horizontally layered anisotropic media. An alternative way is using the numerical methods. JafarGandomi and Takenaka (2007) applied the Radon transform to derive the plane wave equations for vertically heterogeneous isotropic and attenuative media and proposed a staggered-grid finite-difference numerical scheme to simulate plane wave propagation. Recently, they extended this scheme to the case of three-component plane wave (JafarGandomi and Takenaka, 2013).

In this extended abstract, we investigate the plane wave propagation in vertically heterogeneous anisotropic media. The medium is assumed to be lateral homogenous, which means that the horizontal slowness is constant for incident, reflected and transmitted plane waves. First, we review the velocity-stress wave equations in anisotropic media. Then, we derive the velocity-stress formed plane wave equation. Finite-difference method is employed to simulate plane wave propagation, and the corresponding stability condition is derived. Subsequently, we use few numerical examples to show the validity of our scheme and apply it to generate three-component VSP seismograms.

For simplifying vectors and matrices operations, we use the upper-case indices (I , J , K ...) taking the values of 1 or 2, and the lower-case (i , j , k …) taking the values of 1, 2, or 3. ∂_t denotes differentiation with respect to time, Differentiation with respect to spatial coordinate x_l is denoted by ∂_l . The Einstein summation convention over repeated indices is used.

Plane wave equations in vertically heterogeneous, anisotropic media

The time-domain equations for wave propagation in anisotropic media can be found in Carcione (2001). The constitutive relations for general anisotropic media read

$$\partial_t \sigma_{ij} = c_{ijkl} \partial_l \upsilon_k \ , \qquad (1)$$

where υ_i is the particle velocity vector; σ_{ij} is the stress tensor; c_{ijkl} is the fourth-order stiffness tensor, satisfying the symmetry relations,

$$c_{ijkl} = c_{jikl} = c_{ijlk} = c_{klij} \ . \qquad (2)$$

The equations of motion without body force are

$$\rho \partial_t \upsilon_i = \partial_j \sigma_{ij} \ , \qquad (3)$$

where ρ denotes the density. Equations (1) and (3) result in the velocity-stress formed wave equations for numerical modeling of elastic wave propagation in anisotropic media.

For plane wave case, the velocity-stress equations can be rewritten by applying the 2D Radon transformation to the 3D wave equation. The 2D Radon transformation reads

$$f(\tau, p_1, p_2) = \int\int f(t = \tau + p_1 x_1, x_1, x_2) dx_1 dx_2 \ , \qquad (4)$$

where p_1 and p_2 are horizontal projections of slowness vector corresponding to *x* and *y* direction, respectively.

Using the Radon transform, the spatial differentiation with respect to x_1 can be replaced by a temporal differentiation $-p_1 \partial_t$. Hence, equations (1) and (3) become

$$\partial_t \sigma_{ij} = -p_L c_{ijkL} \partial_t \upsilon_k + c_{ijk3} \partial_3 \upsilon_k \ , \qquad (5)$$

$$\rho \partial_t \upsilon_i = -p_J \partial_t \sigma_{iJ} + \partial_3 \sigma_{i3} \ . \qquad (6)$$

Substituting equation (5) into equation (6), then through some algebraic operations, we obtain

$$\partial_t \upsilon_i = \hbar_i(x_3,t) \ , \tag{7}$$

$$\partial_t \sigma_{i3} = -p_L c_{i3kL} \hbar_k(x_3,t) + c_{i3k3}\partial_3 \upsilon_k \ , \tag{8}$$

where

$$\hbar_i(x_3,t) = s_{ij}\left[c_{jMn3} p_M \partial_3 \upsilon_n - \partial_3 \sigma_{n3}\right] \ , \tag{9}$$

$$s_{ij} = (c_{jKiL} p_K p_L - \rho\delta_{ij})^{-1} \ . \tag{10}$$

Equations (7)-(10) form the three-component plane wave equations for vertically heterogeneous anisotropic media. We can see that only three z-axis related stress components are necessary for plane wave in vertically heterogeneous anisotropic media, in addition to three particle velocity components.

Finite Difference Solution

Finite-difference method is used to solve plane wave equations (7)-(10). Partial derivatives are approximated by the finite difference operators. The first-order vertical derivative ∂_z is approximated by N-order finite-difference operator D_z,

$$D_z(f)\big|_{z=0} = \frac{1}{2\Delta z}\sum_{n=1}^{N} a_n (f_n - f_{-n}) \ , \tag{11}$$

where $f_n = f(n\Delta z)$, Δz is vertical sampling, a_n is finite-difference weight (Chu and Stoffa, 2012). Second-order finite-difference operator D_t is adopted to replace temporal derivative ∂_t.

Stationary Condition

Pei et al. (2012) derived the stationary condition for the staggered grid finite-difference method. We adopt their method to derive the stationary condition for our finite-difference scheme.

According to equations (7) and (10), the discretized plane wave equations are written in the following form

$$D_t \boldsymbol{Q} = \mathcal{H} D_z \boldsymbol{Q} \ , \tag{12}$$

where $\boldsymbol{Q} = (\upsilon_1, \upsilon_2, \upsilon_3, \sigma_{13}, \sigma_{23}, \sigma_{33})^T$, the matrix $\mathcal{H}$ is given by

$$\mathcal{H} = \begin{pmatrix} \left(s_{ij} c_{jMn3} p_M\right)_{3\times 3} & \left(-s_{in}\right)_{3\times 3} \\ \left(-p_L c_{i3kL} s_{kj} c_{jMn3} p_M + c_{i3n3}\right)_{3\times 3} & \left(p_L c_{i3kL} s_{kn}\right)_{3\times 3} \end{pmatrix} , \tag{13}$$

where $p_{L(M)}$, $L, M = 1, 2$ are the horizontal slowness projections.

To analyze the stability condition, we assume a uniform infinite anisotropic medium which supports a harmonic plane wave,

$$\boldsymbol{Q} = \boldsymbol{Q}_0 e^{j\omega(t - p_3 z)} \ , \tag{14}$$

where $\boldsymbol{Q}_0 = (\upsilon_1^0, \upsilon_2^0, \upsilon_3^0, \sigma_{13}^0, \sigma_{23}^0, \sigma_{33}^0)^T$ denotes amplitude vector of the harmonic plane wave; p_3 is the vertical slowness projection; ω is the circular frequency.

By inserting equation (14) into the temporal finite-difference operator D_t given in equation (12), we obtain

$$D_t[\boldsymbol{Q}] = j\frac{1}{\Delta t}\sin(\omega\Delta t)\boldsymbol{Q} \ . \tag{15}$$

In a similar way, substituting equation (14) into the spatial finite-difference operator D_z given in equation (12) results in

$$D_z[\boldsymbol{Q}] = -\frac{j}{\Delta z}\sum_{n=1}^{N} a_n \sin(np_3\Delta z)\boldsymbol{Q} \ . \tag{16}$$

We assume that the matrix $\mathcal{H}$ can always be decomposed to

$$\mathcal{H} = \boldsymbol{\Gamma}\boldsymbol{\Lambda}\boldsymbol{\Gamma}^T \ , \tag{17}$$

where $\boldsymbol{\Gamma}$ denotes the eigenvector matrix, $\boldsymbol{\Lambda}$ denotes the eigenvalue diagonal matrix.

Substituting equations (15)-(17) into equation (12), we derive

$$\boldsymbol{\Gamma}\left(\frac{1}{\Delta t}\sin(\omega\Delta t)\boldsymbol{I} + \frac{1}{\Delta z}\sum_{n=1}^{N} a_n \sin(np_3\Delta z)\boldsymbol{\Lambda}\right)\boldsymbol{\Gamma}^T = 0 \ . \tag{18}$$

Consequently, the dispersion relation for the finite-difference scheme is obtained as

$$\sin(\omega\Delta t) = -\frac{\Delta t}{\Delta z}\sum_{n=1}^{N} a_n \sin(np_3\Delta z)\lambda_i \ , \quad i = 1,...,6 \ , \tag{19}$$

where λ_i is the i-th eigenvalue of matrix $\mathcal{H}$.

Considering

$$0 \le \left|\sin(\omega\Delta t)\right| \le 1 \ , \tag{20}$$

and

$$\left|\sum_{m=1}^{N} a_m \sin(np_3\Delta z)\right| \le \sum_{n=1}^{N}|a_n| \ , \tag{21}$$

we obtain the enhanced finite-difference dispersion inequality,

$$\frac{\Delta t}{\Delta z} \le |\lambda|_{\max}^{-1}\left(\sum_{n=1}^{N}|a_n|\right)^{-1} \ , \tag{22}$$

where

$$|\lambda|_{\max} = \max(|\lambda_i|, i = 1,...,6) \ . \tag{23}$$

In general anisotropic media, the expression for λ_i cannot be explicitly derived. For a transversely isotropic medum

with a vertical symmetry axis, the analytical expressions for λ_i, i=1…6, are obtained as

$$\lambda_{1,2}^2 = \frac{b+\sqrt{b^2-4ac}}{2a} \quad , \tag{24}$$

$$\lambda_{3,4}^2 = \frac{b-\sqrt{b^2-4ac}}{2a} \quad , \tag{25}$$

$$\lambda_{5,6}^2 = \frac{\tilde{c}_{44}}{1-\tilde{c}_{66}(p_1^2+p_2^2)} \quad , \tag{26}$$

where eigenvalues $\lambda_{1,2}$, $\lambda_{3,4}$, $\lambda_{5,6}$ correspond to up- and down-going plane qP-, qSV- and qSH-waves, respectively, and

$$a = (1-\tilde{c}_{11}(p_1^2+p_2^2))(1-\tilde{c}_{55}(p_1^2+p_2^2)) \quad , \tag{27}$$

$$b = \tilde{c}_{33}+\tilde{c}_{55}+(\tilde{c}_{13}^2-\tilde{c}_{11}\tilde{c}_{33}+2\tilde{c}_{13}\tilde{c}_{55})(p_1^2+p_2^2) \quad , \tag{28}$$

$$c = \tilde{c}_{33}\tilde{c}_{55} \quad . \tag{29}$$

Here $\tilde{c}_{ij}$ $(i,j=1,2,...,6)$ are the second-order density-normalized elastic moduli in the Voigt notation.

Numerical examples

To demonstrate the validity of finite-difference scheme, we compare the numerical solution with the corresponding analytical solution. A homogeneous tilted transversely isotropic (TTI) model is adopted for numerical test. The tilt of TI symmetry axis is 60^0, and the azimuth of TI symmetry is 45^0. The P- and S-wave on-axis velocities are 3000 m/s and 2000 m/s, respectively. The density is 2.0 g/cm^3. Thomsen parameters are $\varepsilon = 0.3$, $\delta = 0.1$, $\gamma = 0.2$. In this model, the top and bottom boundaries are set to be absorbing ones. The unsplit convolutional perfectly matched layer (CPML) (Komatitish and Martin, 2007) is embedded in our source codes to suppress artificial reflections from these boundaries. A Ricker wavelet with a central frequency of 15 Hz is used to generate the incident qP wave. The dip angle for incident qP wave measured from z axis to the propagation direction is 30^0, and the azimuth of incident wave measured from x-axis to the horizontal projection of TI symmetry axis is 45^0. The temporal sampling is 0.5ms, and spatial sampling is 5 m. The incident qP wave is assigned at the top of the model. The number of spatial samplings is 1000.

The analytical solution for qP wave is

$$\upsilon_i(t,z) = \boldsymbol{g} f(t-p_z z) \, , \quad i=1,2,3 \quad , \tag{30}$$

where υ_i is the i-th component of the particle velocity; $\boldsymbol{g}$ is the unit polarization vector which corresponds to the eigenvector of Christtofel matrix for qP wave; $f(t)$ is the Ricker wavelet.

To examine the accuracy of our scheme, we define the measurement of the relative error in particle velocity as

$$E(t_i) = \frac{\sum_{k=1}^{3}\sum_{j=1}^{M}\left|\upsilon_k(t_i,z_j)-\upsilon_k^s(t_i,z_j)\right|}{\sum_{k=1}^{3}\sum_{j=1}^{M}\left|\upsilon_k^s(t_i,z_j)\right|}\times 100 \quad , \tag{31}$$

where $\upsilon_k(t_i,z_j)$ is the k-th component of particle velocity at time $t=t_i$ and depth $z=z_j$ calculated by numerical method; υ_k^s denotes the k-component of particle velocity for the corresponding analytical solution; M is the number of spatial samplings.

Figure 1 shows the relative error of our FD scheme. One can see the linear increase of relative error from 0 to 0.85 s. After that it starts to oscillate and goes to zero, since anisotropic plane wave begins to reach the absorbing boundary at that time. This Figure indicates that the proposed numerical scheme is only accurate for seismic wave modeling for short traveltime.

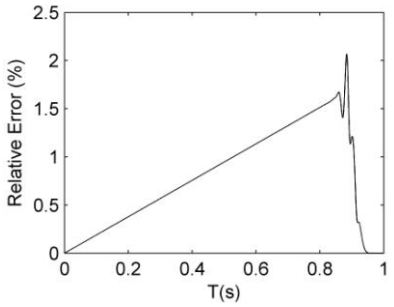

Figure 1. Relative error in particle velocity for our finite-difference scheme.

In the next example, we synthesize the reflection and transmission of plane wave at the interface between an isotropic medium and a horizontal transversely isotropic (HTI) medium. The media parameters for the top isotropic layer are P-wave velocity 2000 m/s, S-wave velocity 1000 m/s, density 2.0 g/cm^3. The TI parameters from previous example are used for the bottom HTI layer. The azimuth of the HTI symmetry axis is 45^0. The whole model was discretized into 800 grids with vertical interval of 5 m. The total number of time samples is 3000 with an interval of 0.5 ms. The interface is located at 1050m depth. A Ricker wavelet used to generate incident P wave is the same as in previous example. The dip and azimuth for incident P wave are also the same as in previous example. CPML is employed to absorb the artificial reflection from the top and bottom of the model.

Figure 2 shows the three component VSP seismograms. One can see that the splitting of transmitted shear wave is very clear. Due to the influence of azimuth of HTI symmetry axis, the reflected SH wave is generated, though its amplitude is much weaker than the one of reflected SV wave. The dip of seismic event corresponds to the apparent velocity along the vertical direction. Hence, the dip information of seismic events can be used to invert the media parameters.

Conclusions

The velocity-stress plane wave equations are derived by applying the Radon transformation to wave equations for vertically heterogeneous anisotropic media. Finite-difference method is employed to solve the plane-wave equations numerically. The corresponding stationary condition is derived. The accuracy of plane wave simulation by the proposed scheme is tested by comparing calculated waveforms to the analytical solution. The proposed plane wave modeling may be used in AVA analysis and waveform inversion for vertically heterogeneous and anisotropic media.

Acknowledgement

We would like to acknowledge the ROSE project for supporting the conference travel.

References

Carcione J.M., 2001, Wave fields in real media: Wave propagation in anisotropic, anelastic and porous media. Elsevier Science Publ. Co., Inc..

Cerveny, V., 2001, Seismic Ray Theory, Cambridge University Press, Cambridge.

Chu, C., and P.L. Stoffa, 2012, Determination of finite-difference weights using scaled binomial windows, Geophysics **77**, W17-W26.

JafarGandomi, A., and H. Takenaka, 2007, Efficient FDTD algorithm for plane-wave simulation for vertically heterogeneous attenuative media. Geophysics **72**, H43–H53.

JafarGandomi, A., and H. Takenaka, 2013, FDTD3C—A FORTRAN program to model multicomponent seismic waves for vertically heterogeneous attenuative media, Computers & Geosciences **51**, 314-323.

Komatitish, D., and R. Martin, 2007, An unsplit convolutional perfectly matched layer improved at grazing incidence for the seismic wave equation. Geophysics **72**, SM155-SM167.

Pei, Z., L.Y. Fu, W. Sun et al., 2012, Anisotropic finite-difference algorithm for modeling elastic wave propagation in fractured coalbeds. Geophysics **77**, C13–C26.

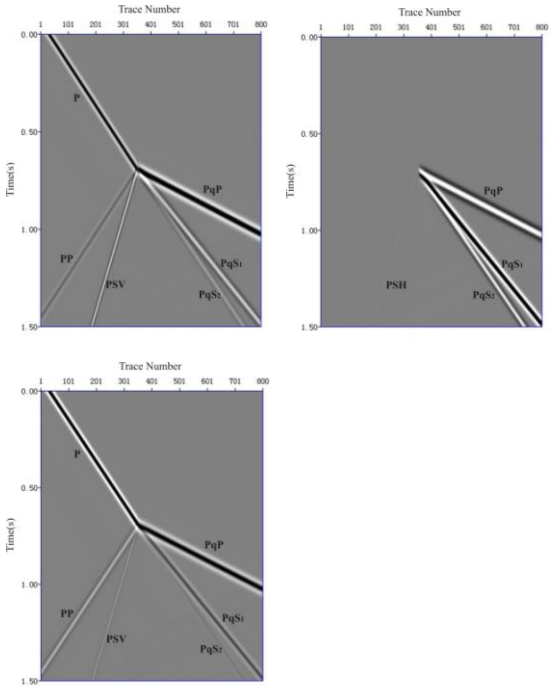

Figure 2. Three-component VSP seismograms (from top-left to bottom-left, x-, y- and z-components of particle velocity, respectively).